

Hammer-shaped slotted antenna design and analysis for wireless applications

Gajendran Srihari¹, Raman Ramamoorthy², Shanmuganantham Thangavelu³, Nimmagadda Padmaja¹

¹Department of Electronics and Communication Engineering, Sree Vidyanikethan Engineering College, Tirupathi, India

²Department of Electronics and Communication Engineering, Aditya College of Engineering, Surampalem, India

³Department of Electronics Engineering, Pondicherry University, Puducherry, India

Article Info

Article history:

Received Jul 6, 2022

Revised Jan 25, 2023

Accepted Jan 26, 2023

Keywords:

Diversity gain

FR4 substrate

Metamaterials

MIMO antenna

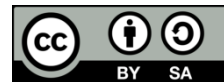
Strip feeding technique

Ultra wideband

ABSTRACT

The method for creating a two-element multiple-input and multiple-output (MIMO) ultra-wideband hammer antenna is presented in this paper. It has been suggested to investigate characteristics of this ultra-wideband antenna design. Split-ring resonators (SRR), made of metamaterial, have enhanced performance of antenna in terms of multiplexing effectiveness, S parameters, radiation characteristics, envelope correlation coefficient, and diversity gain. Reduced weight and size of this antenna technology make it easier to integrate into a 5G and linked object receiver. Because the outputs from the previous designer to the target entity did not satisfy the standards, we thoroughly researched design attributes and made parametric changes to the design to reach the precise outcomes.

This is an open access article under the [CC BY-SA](https://creativecommons.org/licenses/by-sa/4.0/) license.



Corresponding Author:

Gajendran Srihari

Department of Electronics and Communication Engineering, Sree Vidyanikethan Engineering College
Tirupathi, Andhra Pradesh-517 102, India

Email: srihari.g@vidyanikethan.edu

1. INTRODUCTION

High channel capacities and data transmission speeds became major research concerns as wireless communication systems advanced. Limiting the transmission's data rate and channel multipath fading are the two difficulties encountered. A strong resistance to the idea of high-speed transmission and multipath fading ability may be seen in ultra-wideband technology (UWB) [1]. For high-speed wireless communication and short-range transmission, UWB is regarded as the optimal information carrier due to its benefits of great penetration capabilities, low power spectrum density and precise location. Multiple-input and multiple-output (MIMO) technology achieves an important increase in high transmission rate and channel capacity comparative to the number of antennas employing multiple antennas at the transmitter and receiver using spatial diversity and multipath transmission impact of the channel. Large channel capacity and high data transmission rates can be attained while preventing multipath fading effects by combining UWB with MIMO technologies [2].

The poor coupling of the antennas is the fundamental issue with UWB MIMO antennas. Portable terminals and wireless devices are getting smaller and more integrated as a result of the quick development of modern mobile communications. UWB MIMO miniaturisation allows UWB MIMO antennas get smaller, their physical separation gets closer, and their mutual coupling gets stronger. This causes electromagnetic interference to get worse and worse, which breaks down the antenna. Therefore, one of the main concerns in UWB MIMO antenna development is how to improve cell-to-cell isolation. Creating decoupling structures [3], [4], cutting slits [5] loading metamaterials, decoupling frequency-selective surfaces [6], electromagnetic bandgap structures [7]–[9], neutralisation lines [10]–[13], and parasitic cell decoupling [14], as well as

erroneous grounding structures [15], [16] and polarisation diversity techniques [17]–[19], are typical methods to increase MIMO antenna isolation. The isolation between cells is effectively increased to more than 2 dB using two-port MIMO antenna [3] uses a "T"-shaped separation structure between cells, but bandwidth is only 2.33-6.71 GHz, and the size is too huge. Size of the two-port MIMO [5] antenna is 7 mm, 93 mm, and 1.6 mm; however, it runs between 3.1 and 10.6 GHz and attains a decent isolation of 31 dB by etching the ground plate's central slot. Average isolation degree of the antenna in working region is more than 26 dB in MIMO antenna [10], which also has a working bandwidth increase from 2.1 to 20 GHz, but a low envelope correlation coefficient (ECC) antenna and an excessively big size. The compact four-port MIMO antenna in [12] has a frequency range of 3-13.5 GHz and a small construction.

Cylinder approximation method is mostly used to estimate the minimum resonant frequency in the case of monopole antenna whose radiation pattern is with regular shapes [20], [21] so the size of the radiation pattern and ground is adjusted approximately. Also, the isolation can be enhanced by making a slot etched on a T-shaped antenna [22]. For a MIMO system the ECC of all the ports should be less than 0.002 satisfying the requirements of MIMO antenna correlation parameters [23]. By using ECC another important parameter namely diversity gain can be calculated for a MIMO antenna [24]. The total efficiency of the MIMO system in a multipath fading environment can be calculated by the parameter mean effective gain (MEG) [25]. In conclusion, the antennas from the aforementioned references have complex construction, poor isolation, and enormous diameters.

Here, we suggest a UWB antenna that operates in 7.8 GHz band, has an efficiency of more than 89%, and a gain between 6 and 9.5 dB. Measurements of reflection parameter at antenna's input are found to be in good agreement with the calculations. The next solution we suggest has two extremely close antennas that are spaced at $\lambda/12$. Consequence of mutual coupling can be reduced down to 35 dB at 7.8 GHz with an isolation gain of 20 dB when five SRR cells are introduced and placed linearly among two radiating elements. This is in comparison to two antennas without SRR. The transmission parameter S21 is the subject of a comparison between models and measurements in this research. As a result, it can be seen that suggested UWB MIMO multi-antenna system is strong contender for future wireless communication technologies like 5G and linked objects.

2. METHOD: ANTENNA CONFIGURATION AND THEORETICAL ANALYSIS

A transparent view of antenna design is shown in Figure 1. As can be seen, the antenna structure consists of a ground plane with a square-ring slot and two rectangular microstrip lines placed on opposite top sides of the slot resonator. Furthermore, the square-ring slot resonator on the antenna's upper layer is crossed by a pair of parasitic devices. The antenna is 1.6 mm thick and has a modest profile. Table 1 lists the parameter values for the single-element antenna.

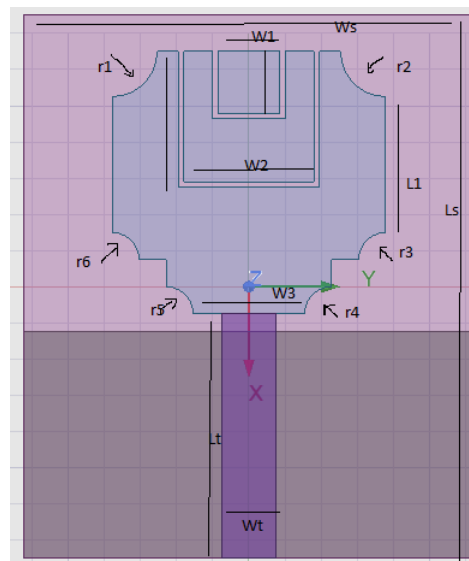


Figure 1. Base antenna design front view and back view with dimension parameters. Geometry of proposed design ($L_s=30$ mm, $W_s=25$ mm, $L_g=12.5$ mm, $H_s=1.6$ mm, $W_t=3.6$ mm, $N=2.4$ mm, $I=0.75$ mm, $L_t=2.3$ mm, $W_f=3$ mm, $W_1=3.4$ mm, $L_1=7.5$ mm, $r_1=r_2=2.5$ mm, $r_3=r_4=r_5=r_6=1.5$, $W_2=7.2$, $F=0.3$)

Table 1. Design parameters of antenna

Parameter	Value (mm)
Ws	25
L	30
hs	1.6
Lg	12.5
Lt	2.3
r ₁ =r ₂	2.5
r ₃ =r ₄ =r ₅ =r ₆	1.5

The patch was designed for internet of thing (IoT) applications; hence 7.8 GHz was chosen as the operating frequency (f_0). The antenna's maximum usable height is 1.6 mm. Its value is between 0.8 mm and 1.6 mm. Consequently, the substrate is 1.6 mm thick or 1.6 mm tall (h). Consider the substrate material, FR4, which has a relative permittivity of 4.4 (ϵ_r). Width of substrate is given by the (1).

$$W_s = \frac{1}{2f_0\sqrt{\mu_0\epsilon_0}} \sqrt{\frac{2}{\epsilon_r+1}} \quad (1)$$

By the (1), the width of the substrate as 38.04 mm (W). Effective dielectric constant is given by the (2).

$$\epsilon_{reff} = \frac{\epsilon_r+1}{2} + \frac{\epsilon_r-1}{2} \left[1 + 12 \frac{h}{W} \right]^{-\frac{1}{2}} \quad (2)$$

By the (2), the effective dielectric constant as 4.08 (ϵ_{reff}). The margins of the patch do not mark the end of the electric fields. The electric field radiates down the z axis, whereas the magnetic field exists in the x, y plane. Due to these neighboring fields, patch appears electrically larger than its true size. The letters L and, respectively, denote the effective dielectric constant $reff$, the ratio W/h , and the increase in the patch's diameter along its path.

$$\frac{\Delta L}{h} = 0.412 \left[\frac{(\epsilon_{reff}+0.3)\left(\frac{W}{h}+0.264\right)}{(\epsilon_{reff}-0.288)\left(\frac{W}{h}+0.8\right)} \right] \quad (3)$$

From the (3), the increase in dimension of patch is 0.723 mm (ΔL). Length of substrate is given by the (4).

$$L_s = \frac{1}{2f_0\sqrt{\epsilon_{reff}\mu_0\epsilon_0}} - 2\Delta L \quad (4)$$

From the (4), the length of the substrate as 30 mm (L_s). The feed should have a width that is 1/4 to 1/5 the width of the substrate. Consequently, the feed's width is 3 mm (W_f). Placement of the defective ground structure from the L and W of the ground by $\lambda/4, n\lambda/4$. Therefore, the deficient ground structure's width and length are 25 and 30 mm, respectively.

3. MIMO SYSTEM'S CHARACTERISTICS

A single-band antenna setup created exclusively to cover UWB. This system has two components and is of the enormous MIMO variety. The presence of two power ports is required. In order to accomplish this, initially, we developed a reference system with two ultra low band (ULB) antennas. Geometry of two similar MIMO-UWB antenna elements first presented in Figure 2 which is mounted on a printed circuit board (PCB) with the dimensions $l_{sub} \times W_{sub}=35 \times 48 \text{ mm}^2$. These two pieces are separated by $d=16.8 \text{ mm}$, it should be noted (centre to centre).

To provide effective impedance matching across a range of frequencies, a shared ground plane that has been somewhat truncated is used at the back of the substrate. The results of reflecting coefficient optimization for antenna 1's characteristics are $L_{sub}=35 \text{ mm}$, $L_{gnd}=12.5 \text{ mm}$, $W_{sub}=48 \text{ mm}$, and $L_f=13.5 \text{ mm}$. Results demonstrate the antenna's S parameters, S_{11} as calculated and tested (antenna 2 is acceptable for 50 Ohms). The difference between them at about 2.1 GHz is mostly brought on by losses in the measurement wire, and they generally concur. An important feature of this antenna is its capacity to operate between 2 and 18 GHz (counting industrial scientific medical (ISM) 2.45 GHz and UWB bands).

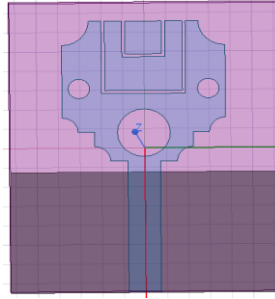


Figure 2. Base antenna design

4. RESULTS AND DISCUSSION

The reflection coefficient, voltage standing wave ratio (VSWR), gain, directivity and radiation pattern of base antenna were all modeled using HFSS tool. Return loss compares the power reflected by the antenna with the power supplied into it by the transmission line, is a logarithmic ratio expressed in decibels (dB). Antenna has return loss of -28 dB, -17.49 dB at frequencies 5.8 GHz and 10.1 GHz and from 5.2 to 6.4 GHz and 9.4 to 10.7 GHz return loss $S(1,1)$ is below -10 dB as shown in Figure 3. The efficiency with which radio-frequency power is carried from power source, through transmission line, and into load is measured by the VSWR. According to Figure 4, the VSWR for designed antennas is 1.1540 at a frequency of 7.8 GHz.

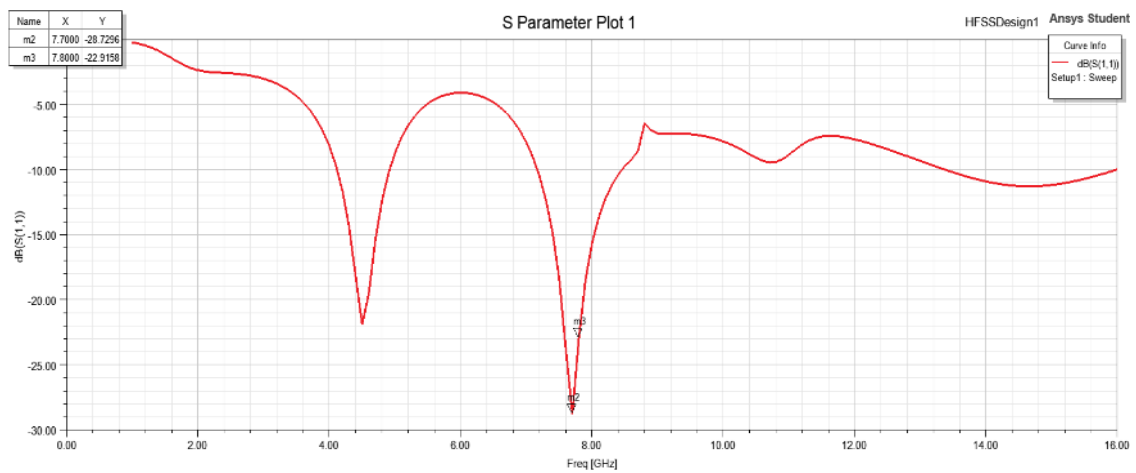


Figure 3. Base antenna simulated reflection coefficient at 7.8 GHz

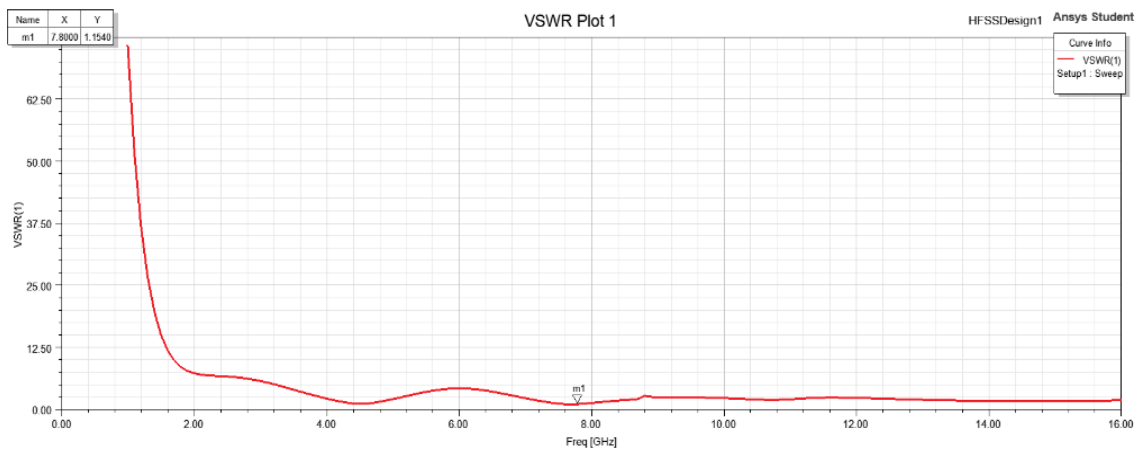


Figure 4. Base antenna simulated VSWR at 7.8 GHz

As shown in Figure 5, the gain for designed antennas is 8.5 dB at a frequency of 7.8 GHz, in Figure 6, the directivity for designed antennas is 8.5 dB at a frequency of 7.8 GHz. Figure 7 shows E-plane pattern and Figure 8 shows H-plane pattern of base antenna design. Figure 9 represents the schematic of 1×2 microstrip antenna.

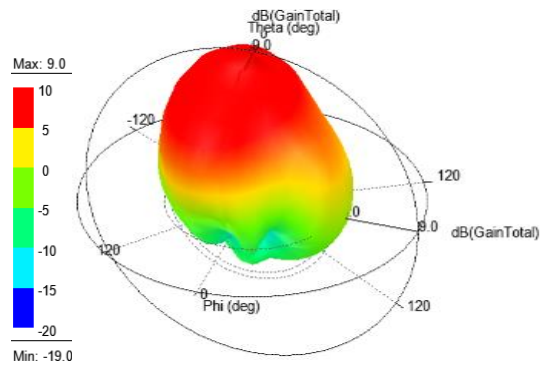


Figure 5. Base antenna gain at 7.8 GHz

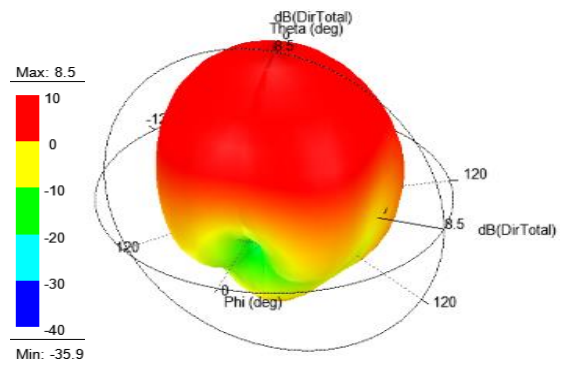


Figure 6. Base antenna directivity at 7.8 GHz

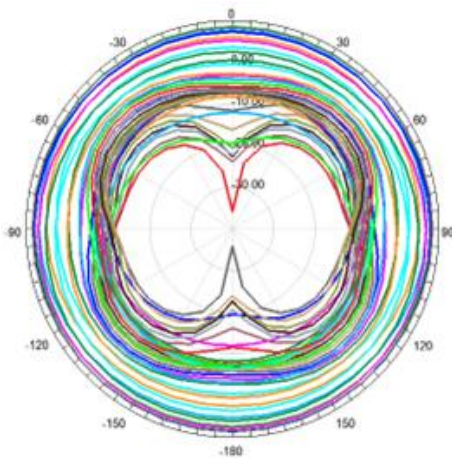


Figure 7. Base antenna E-plane pattern

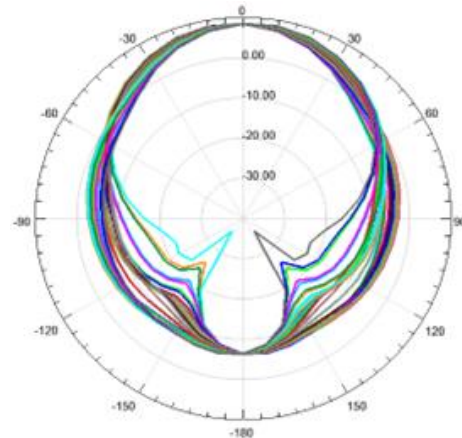


Figure 8. Base antenna H-plane pattern

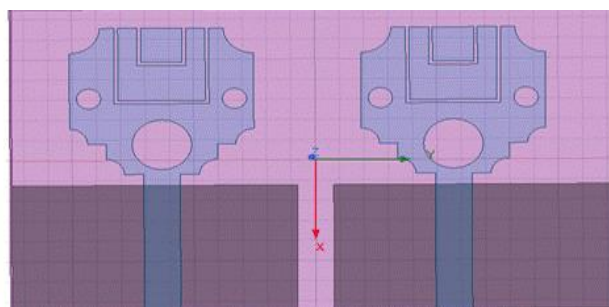


Figure 9. Antenna design of 1×2 microstrip antenna

Return loss, which contrasts the power transmitted into the antenna from the transmission line with power reflected by the antenna, is logarithmic ratio expressed in decibels (dB). The return loss has improved as compared to the previous design and received output isn't sufficient to the market conditions, leads to improve the results some better. The antenna takes return loss of -21.7 dB at frequencies 7.8 GHz return loss $S(1,1)$ is below -10 dB as shown in Figure 10.

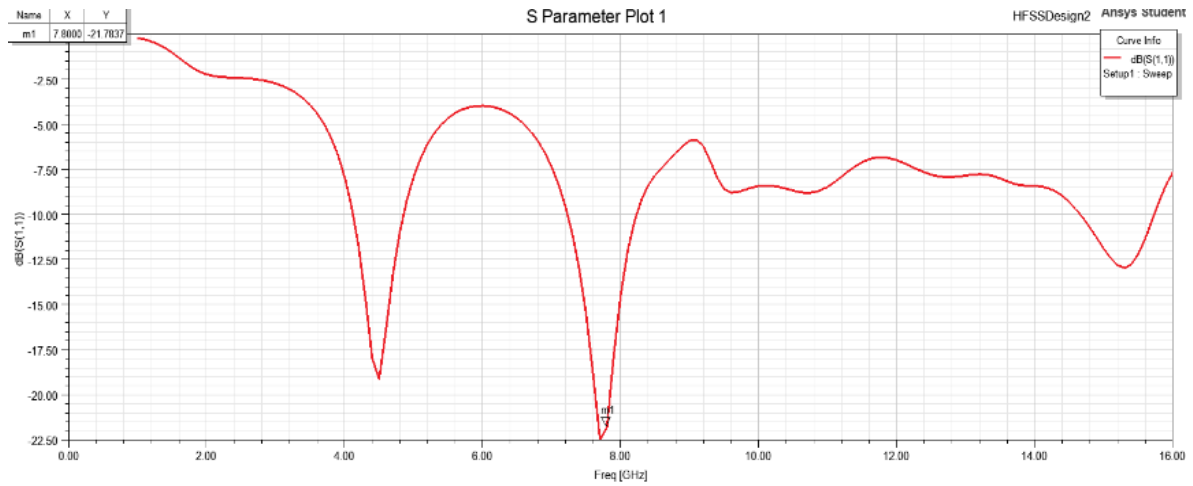


Figure 10. Returnloss of proposed 1x2 microstrip antenna

Efficiency with which radio-frequency power is carried from power source, through transmission line, and into a load is measured by VSWR. For designed antennas VSWR is 1.173 at a frequency of 7.8 GHz as shown in Figure 11. Figure 12, the gain for designed 1x2 microstrip antenna gain is 8.9 dB at a frequency of 7.8 GHz and the directivity is 9 dB at a frequency of 7.8 GHz. Figure 13 shows 2D radiation pattern for E-plane and H-Plane of 1x2 microstrip antenna design. Figure 14 shows 2x2 microstrip antenna design.

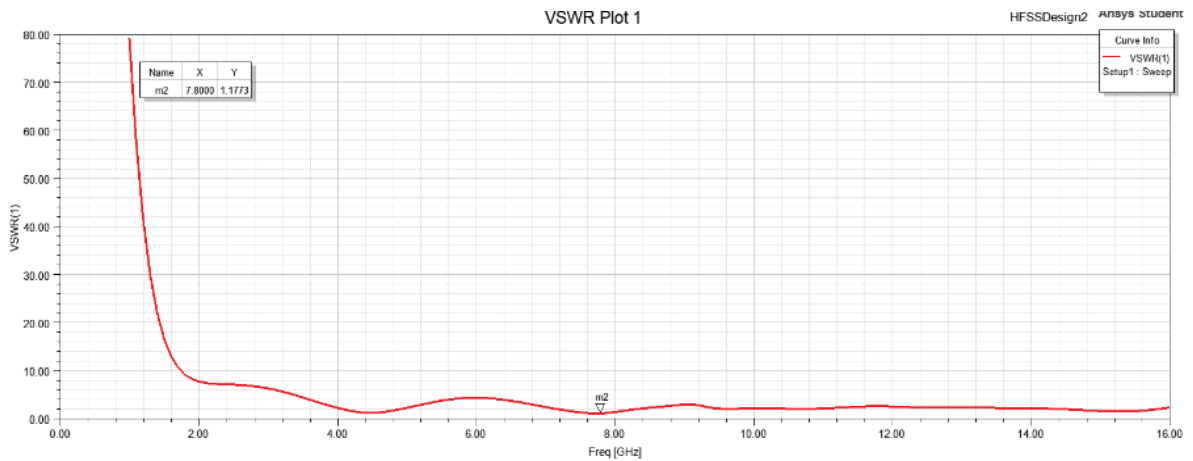


Figure 11. VSWR of proposed 1x2 microstrip antenna

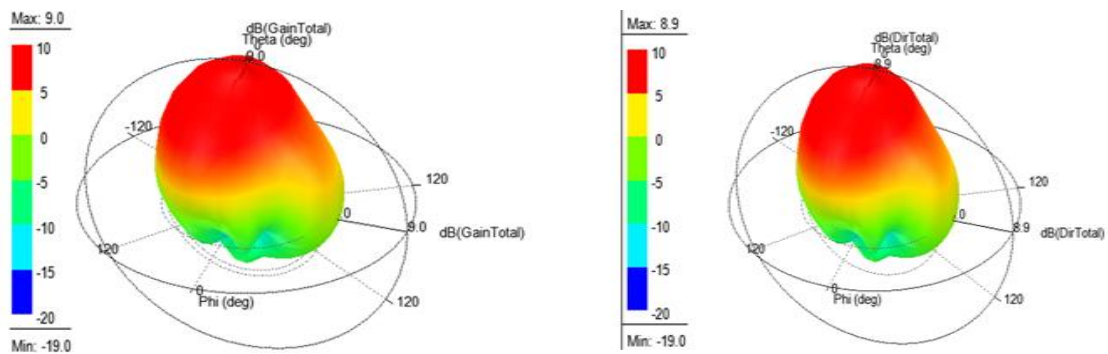


Figure 12. 3D polar plot diagram for the proposed 1x2 microstrip antenna gain at 7.8 GHz and antenna directivity at 7.8 GHz

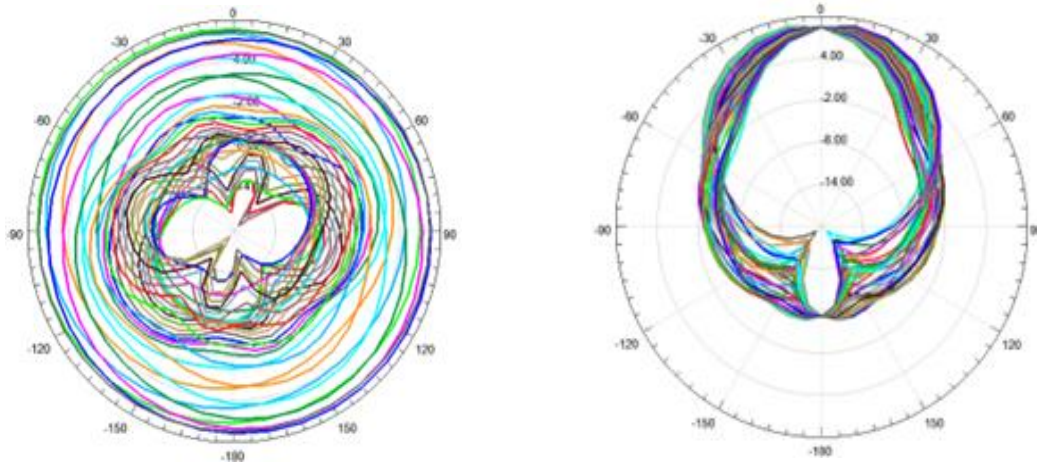


Figure 13. Proposed 1×2 microstrip antenna E-plane and H-plane 2D radiation pattern

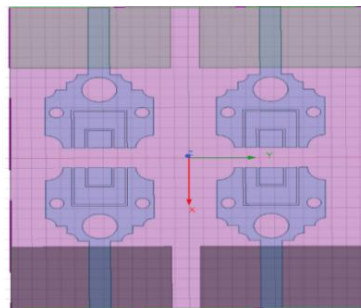


Figure 14. 2×2 antenna design of microstrip antenna

Return loss, which contrasts the power transmitted into the antenna from the transmission line with the power reflected by the antenna, is logarithmic ratio expressed in decibels (dB). The antenna has return loss of -28 dB, -17.49 dB at frequencies 5.8 GHz and 10.1 GHz and From 5.2 GHz to 6.4 GHz and 9.4 GHz to 10.7 GHz return loss $S(1,1)$ is below -10 dB as shown in Figure 15.

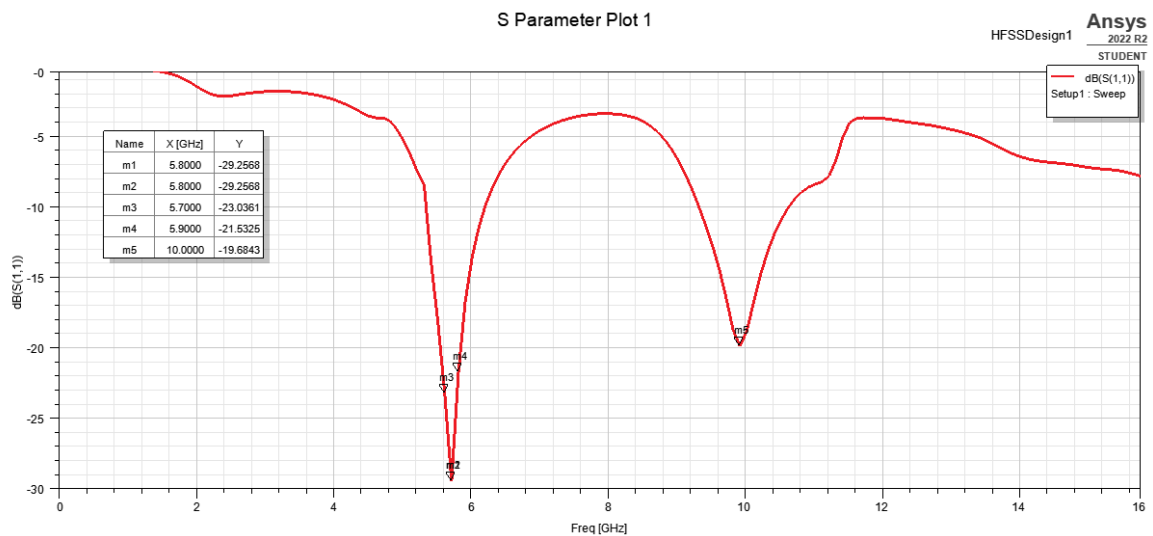


Figure 15. Simulated return loss $S(1,1)$ of proposed 2×2 microstrip antenna

The efficiency with which radio-frequency power is carried from power source, through transmission line, and into load is measured by VSWR. For designed antennas VSWR is 1.0869 at a frequency of 7.8 GHz as shown in Figure 16. Figure 17 represents polar plots 2×2 microstrip antenna gain at 7.8 GHz. Figure 17(a) gives gain at 7.8 GHz. Figure 17(b) gives directivity at 7.8 GHz of 2×2 microstrip antenna. Figure 18 shows 2D radiation pattern of 2×2 antenna in E-plane and H-plane.

The Table 2 shows the simulated performance characteristics with improved reflection coefficient as -27.61 dB. Voltage Standing Wave Ratio at 7.8 GHz is 1.08. Similarly the 2×2 antenna design give better directivity and gain at gain as 9.5 dB and 9.4 dB respectively.

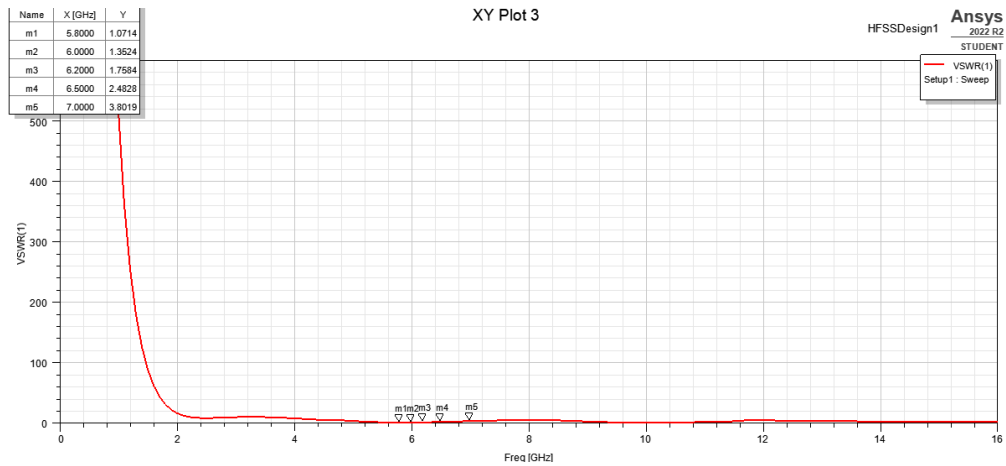


Figure 16. Simulated VSWR of proposed 2×2 microstrip antenna

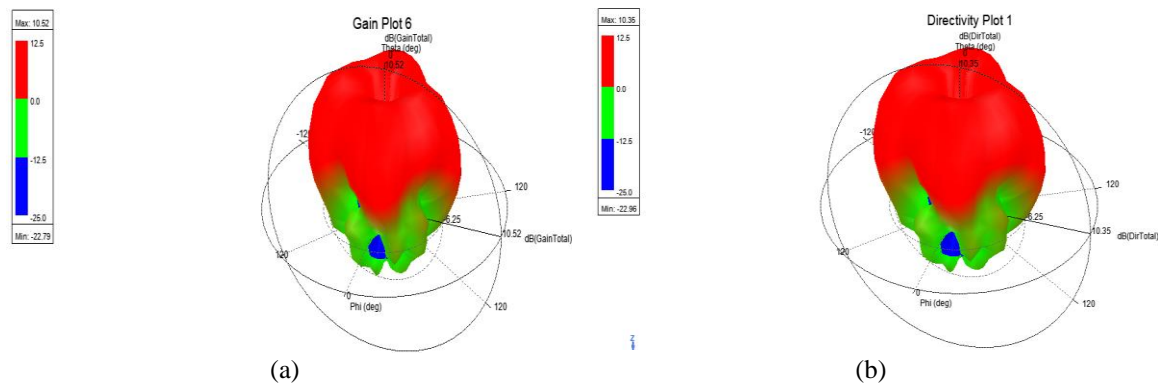


Figure 17. 3D polar plot diagram for the proposed 2×2 microstrip antenna (a) gain at 7.8 GHz and (b) directivity at 7.8 GHz

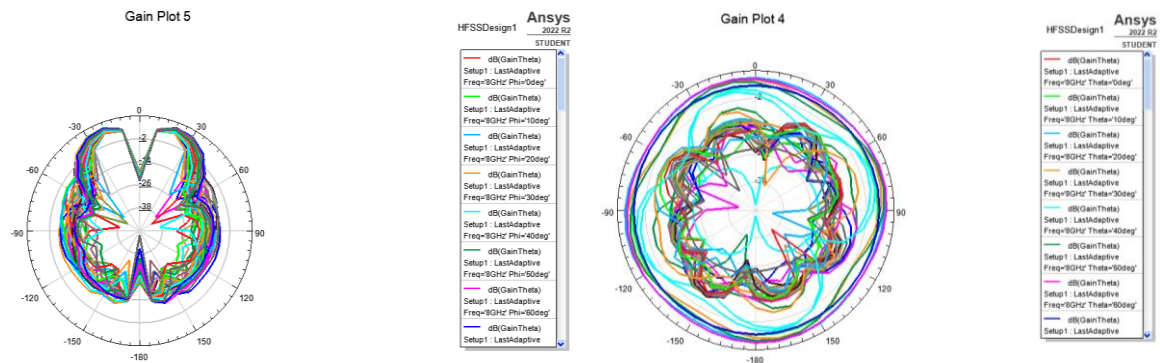


Figure 18. 2D radiation pattern of proposed 2×2 antenna E-plane pattern and H-plane pattern

Table 2. Design parameters of antenna

Parameter	Antenna-1	Antenna-2 [1X2]	Antenna-3 [2X2]
Frequency [GHz]	7.8	7.8	7.8
S(1,1) [dB]	-22	-21.7837	-27.61
VSWR	1.154	1.173	1.08
Gain [dB]	8.5	9.0	9.5
Directivity [dB]	8.5	8.9	9.4

5. CONCLUSION

HFSS software is used to develop and simulate a rubber hard based MIMO antenna for endless wireless applications. At 7.8 GHz, the developed antenna obtained good gain, return loss, and VSWR. The completed system's modeling findings validated the benefits of the Rubber Hard based antenna for wireless applications, making it a strong contender for wireless communications systems like 5G and linked devices. The design's minor results are only revealed through simulation results. We can proceed with the manufacture of the proposed MIMO antenna using these MIMO antenna results. Due to factors such as fabrication material purity, measurement considerations, and atmosphere, the results may or may not match the simulated results after fabrication. HFSS software is used to build and model MIMO antennas for wireless applications. The antenna has a modeling good return loss of less than -10 dB at 7.8 GHz, planned antenna has good VSWR and return loss. Proposed antenna design is suitable for a range of 7.8 GHz wireless applications. This facilitates their interaction with telecommunications systems.




REFERENCES

- [1] B. Mohamadzade, R. B. V. B. Simorangkir, R. M. Hashmi, and A. Lalbakhsh, "A conformal ultrawideband antenna with monopole-like radiation patterns," *IEEE Transactions on Antennas and Propagation*, vol. 68, no. 8, pp. 6383–6388, Aug. 2020, doi: 10.1109/TAP.2020.2969744.
- [2] R. Chandel, A. K. Gautam, and K. Rambabu, "Tapered fed compact UWB MIMO-diversity antenna with dual band-notched characteristics," *IEEE Transactions on Antennas and Propagation*, vol. 66, no. 4, pp. 1677–1684, Apr. 2018, doi: 10.1109/TAP.2018.2803134.
- [3] A. Kumar, A. Q. Ansari, B. K. Kanaujia, and J. Kishor, "A novel ITI-shaped isolation structure placed between two-port CPW-fed dual-band MIMO antenna for high isolation," *AEU - International Journal of Electronics and Communications*, vol. 104, pp. 35–43, May 2019, doi: 10.1016/j.aeue.2019.03.009.
- [4] L. Wang *et al.*, "Compact UWB MIMO antenna with high isolation using fence-type decoupling structure," *IEEE Antennas and Wireless Propagation Letters*, vol. 18, no. 8, pp. 1641–1645, Aug. 2019, doi: 10.1109/LAWP.2019.2925857.
- [5] A. H. Radhi, R. Nilavalan, Y. Wang, H. S. Al-Raweshidy, A. A. Eltokhy, and N. Ab Aziz, "Mutual coupling reduction with a wideband planar decoupling structure for UWB-MIMO antennas," *International Journal of Microwave and Wireless Technologies*, vol. 10, no. 10, pp. 1143–1154, Dec. 2018, doi: 10.1017/S1759078718001010.
- [6] M. Bilal *et al.*, "A miniaturized FSS-based eight-element MIMO antenna array for off/on-body WBAN telemetry applications," *Electronics*, vol. 11, no. 4, Feb. 2022, doi: 10.3390/electronics11040522.
- [7] S. Modak and T. Khan, "A slotted UWB-MIMO antenna with quadruple band-notch characteristics using mushroom EBG structure," *AEU - International Journal of Electronics and Communications*, vol. 134, May 2021, doi: 10.1016/j.aeue.2021.153673.
- [8] N. Jaglan, S. D. Gupta, B. K. Kanaujia, S. Srivastava, and E. Thakur, "Triple band notched DG-CEBG structure based UWB MIMO/diversity antenna," *Progress In Electromagnetics Research C*, vol. 80, pp. 21–37, 2018, doi: 10.2528/PIERC17090702.
- [9] A. Khan, S. Bashir, S. Ghafoor, and K. K. Qureshi, "Mutual coupling reduction using ground stub and EBG in a compact wideband MIMO-antenna," *IEEE Access*, vol. 9, pp. 40972–40979, 2021, doi: 10.1109/ACCESS.2021.3065441.
- [10] V. S. D. Rekha, P. Pardhasaradhi, B. T. P. Madhav, and Y. U. Devi, "Dual band notched orthogonal 4-element MIMO antenna with isolation for UWB applications," *IEEE Access*, vol. 8, pp. 145871–145880, 2020, doi: 10.1109/ACCESS.2020.3015020.
- [11] S. Kumar, G. H. Lee, D. H. Kim, W. Mohyuddin, H. C. Choi, and K. W. Kim, "Multiple-input-multiple-output/diversity antenna with dual band-notched characteristics for ultra-wideband applications," *Microwave and Optical Technology Letters*, vol. 62, no. 1, pp. 336–345, Jan. 2020, doi: 10.1002/mop.32012.
- [12] A. A. Khan, S. A. Naqvi, M. S. Khan, and B. Ijaz, "Quad port miniaturized MIMO antenna for UWB 11 GHz and 13 GHz frequency bands," *AEU - International Journal of Electronics and Communications*, vol. 131, Mar. 2021, doi: 10.1016/j.aeue.2021.153618.
- [13] R. N. Tiwari, P. Singh, B. K. Kanaujia, and K. Srivastava, "Neutralization technique based two and four port high isolation MIMO antennas for UWB communication," *AEU - International Journal of Electronics and Communications*, vol. 110, Oct. 2019, doi: 10.1016/j.aeue.2019.152828.
- [14] W. Mu *et al.*, "A flower-shaped miniaturized UWB-MIMO antenna with high isolation," *Electronics*, vol. 11, no. 14, Jul. 2022, doi: 10.3390/electronics11142190.
- [15] A. K. Sohi and A. Kaur, "A complementary Sierpinski gasket fractal antenna array integrated with a complementary Archimedean defected ground structure for portable 4G/5G UWB MIMO communication devices," *Microwave and Optical Technology Letters*, vol. 62, no. 7, pp. 2595–2605, Jul. 2020, doi: 10.1002/mop.32356.
- [16] L. Wu, X. Cao, and B. Yang, "Design and analysis of a compact UWB-MIMO antenna with four notched bands," *Progress In Electromagnetics Research M*, vol. 108, pp. 127–137, 2022, doi: 10.2528/PIERM21112101.
- [17] S. Rajkumar, A. Anto Amala, and K. T. Selvan, "Isolation improvement of UWB MIMO antenna utilizing molecule fractal structure," *Electronics Letters*, vol. 55, no. 10, pp. 576–579, May 2019, doi: 10.1049/el.2019.0592.
- [18] A. A. Khan *et al.*, "Printed closely spaced antennas loaded by linear stubs in a MIMO style for portable wireless electronic devices," *Electronics*, vol. 10, no. 22, Nov. 2021, doi: 10.3390/electronics10222848.
- [19] S. Agarwal, U. Rafique, R. Ullah, S. Ullah, S. Khan, and M. Donelli, "Double overt-leaf shaped CPW-fed four port UWB MIMO antenna," *Electronics*, vol. 10, no. 24, p. 3140, Dec. 2021, doi: 10.3390/electronics10243140.




- [20] P. Mezzanotte, L. Roselli, and R. Sorrentino, "A simple way to model curved metal boundaries in FDTD algorithm avoiding staircase approximation," *IEEE Microwave and Guided Wave Letters*, vol. 5, no. 8, pp. 267–269, 1995, doi: 10.1109/75.401071.
- [21] N. Telzhensky and Y. Leviatan, "Novel method of UWB antenna optimization for specified input signal forms by means of genetic algorithm," *IEEE Transactions on Antennas and Propagation*, vol. 54, no. 8, pp. 2216–2225, Aug. 2006, doi: 10.1109/TAP.2006.879201.
- [22] Z. He, J. Jin, Y. Zhang, and Y. Duan, "Design of a two-dimensional 'T' shaped metamaterial with wideband, low loss," *IEEE Transactions on Applied Superconductivity*, vol. 29, no. 2, pp. 1–4, Mar. 2019, doi: 10.1109/TASC.2018.2889356.
- [23] K. S. Sultan and H. H. Abdullah, "Planar UWB MIMO-diversity antenna with dual notch characteristics," *Progress In Electromagnetics Research C*, vol. 93, pp. 119–129, 2019, doi: 10.2528/PIERC19031202.
- [24] A. Iqbal, O. A. Saraereh, A. W. Ahmad, and S. Bashir, "Mutual coupling reduction using f-shaped stubs in UWB-MIMO antenna," *IEEE Access*, vol. 6, pp. 2755–2759, 2018, doi: 10.1109/ACCESS.2017.2785232.
- [25] A. A. Khan *et al.*, "Design of a dual-band MIMO dielectric resonator antenna with pattern diversity for WIMAX and WLAN applications," *Progress In Electromagnetics Research M*, vol. 50, pp. 65–73, 2016, doi: 10.2528/PIERM16070102.

BIOGRAPHIES OF AUTHORS






Gajendran Srihari    received B.Tech. Degree in Electronics and Communication Engineering from JNTU Hyderabad, M.Tech. Degree in VLSI System Design from JNTU Hyderabad and Ph.D. in the area of MEMS from Pondicherry Central University under the guidance of Dr. T. Shanmuganatham, Professor, Pondicherry Central University, from Pondicherry. His research interest includes antennas, MEMS/NEMS. He is currently working as Associate Professor in srividyanikethan Engineering College, Andhra Pradesh. He can be contacted at email: srihari.nan@gmail.com.






Raman Ramamoorthy    received B.E. degree in Electronics and Communication Engineering from Anna University, M.Tech. Degree in Electronics and Communication Engineering from Pondicherry University. He has completed his Ph.D. in the area of RF MEMS under the guidance of Dr. T. Shanmuganatham. He has four years of teaching experience. Currently He is working as Associate Professor at Aditya College of Engineering, Surampalem, East Godavari District. His research interest includes RF MEMS and antennas. He is a life member of ISTE and IETE. He can be contacted at email: ramanphdr@gmail.com.



Dr. Shanmuganatham Thangavelu    is working as a teaching and research faculty in the Department of Electronics Engineering at Pondicherry University. He received the B.E. degree in Electronics and Communication Engineering from University of Madras, M.E. degree in Communication Engineering from Madurai Kamaraj University and Ph.D. degree (Received Gold Medal for Best Thesis) in the field of Antenna Engineering from National Institute of Technology (NIT), Tiruchirappalli. His research interest includes antennas, microwave/millimetre-wave engineering and MEMS/NEMS, satellite, space, and wireless industries. He can be contacted at email: shanmuga.dee@pondiuni.edu.in.



Dr. Nimmagadda Padmaja    received B E (ECE) from University of Mumbai, India, M Tech and Ph.D from S V University in the area of Atmospheric Radar Signal Processing in 2012. Currently she is working as Professor in Sree Vidyanikethan Engineering College (Autonomous), Tirupati, India. Her areas of interests include signal and image processing, communication systems. She can be contacted at email: padmaja.n@vidyanikethan.edu.